



Nanoscale

**Orbital design of topological insulators from two-dimensional semiconductors**

Journal:	<i>Nanoscale</i>
Manuscript ID	NR-COM-08-2019-006859.R1
Article Type:	Communication
Date Submitted by the Author:	27-Sep-2019
Complete List of Authors:	Gao, Lei; Chinese Academy of Sciences Institute of Physics, Sun, Jiatao; Chinese Academy of Sciences Institute of Physics Sethi, Gurjyot; University of Utah, Department of Materials Science Zhang, Yu-Yang; University of the Chinese Academy of Sciences, School of Physical Sciences Du, Shixuan; Chinese Academy of Sciences Institute of Physics Liu, Feng; University of Utah, Department of Materials Science

SCHOLARONE™  
Manuscripts

# Orbital design of topological insulators from two-dimensional semiconductors

Lei Gao<sup>†, #</sup>, Jia-Tao Sun<sup>†, §, #</sup>, Gurjyot Sethi<sup>‡</sup>, Yu-Yang Zhang<sup>†, //</sup>, Shixuan Du<sup>†, //, \*</sup>, Feng Liu<sup>‡, \*</sup>

<sup>†</sup> Institute of Physics & University of Chinese Academy of Sciences, Chinese Academy of Sciences, Beijing 100190, P.R. China

<sup>‡</sup> Department of Materials Science and Engineering, University of Utah, Salt Lake City, Utah 84112, USA

<sup>§</sup>School of Information and Electronics, Beijing Institute of Technology, Beijing 100081, China

<sup>//</sup> CAS Center for Excellence in Topological Quantum Computation, Beijing 100190, P.R. China

<sup>#</sup>Contributed equally

<sup>\*</sup>Corresponding author. E-mail: [sxdu@iphy.ac.cn](mailto:sxdu@iphy.ac.cn); [fliu@eng.utah.edu](mailto:fliu@eng.utah.edu)

Two-dimensional (2D) materials have attracted much attention because they exhibit various intrinsic properties, which are, however, usually not interchangeable. Here we propose a generic approach to convert 2D semiconductors to 2D topological insulators (TIs) via atomic adsorption. The approach is underlined by an orbital design principle that involves introducing an extrinsic *s*-orbital state of the adsorbate into the intrinsic *sp*-bands of a 2D semiconductor, so as to induce *s-p* band inversion for a TI phase, as demonstrated by tight-binding model analyses. Based on first-principles calculations, we successfully apply this approach to convert CuS, CuSe and CuTe into TIs by adsorbing Na, Na<sub>0.5</sub>K<sub>0.5</sub> and K as well as Rb and Cs one adatom per unit cell. Moreover, if the chalcogens in the 2D semiconductor have a decreasing ability of accepting electrons, the adsorbates should have an increasing ability of donating electrons. Our findings open a new door to discovering TIs by predictive materials design beyond finding preexisting TIs.

Recently, two-dimensional (2D) materials have attracted much attention for both fundamental interest and their potential applications.<sup>1-4</sup> So far, a suite of different classes of 2D materials have been discovered, ranging, e.g., from inorganic Dirac semimetal,<sup>5, 6</sup> semiconductor,<sup>7, 8</sup> topological insulator (TIs),<sup>9-12</sup> superconductor<sup>13</sup> and ferromagnet,<sup>14</sup> to their organic counterparts<sup>15-18</sup>. Although some efforts have also been made to tune the intrinsic properties of 2D materials, such as by strain<sup>19</sup> and alloying<sup>20</sup>, usually different classes of 2D materials are not interchangeable. Here we propose a generic approach to convert 2D semiconductors, which are amply abundant, to 2D TIs, which are relatively less available, via surface adsorption and strain engineering.

Because of a very large surface area, 2D materials are extremely sensitive to surface modification;<sup>21, 22</sup> while their ultrathinness makes them very sensitive to strain.<sup>22-24</sup> This offers them a unique advantage over their 3D counterparts, as the intrinsic properties of the whole 2D materials can in principle be modified through adsorption and/or strain engineering so that one class of 2D materials may be converted into another class. Below we demonstrate this possibility by converting 2D semiconductors into TIs predominantly by surface adsorption where one alkali atom is introduced into each unit cell of the 2D semiconductor to completely change its intrinsic band structure and band topology, which is apparently impossible for 3D materials.

We will first illustrate our approach, which is underlined by an orbital design principle, using a tight-binding (TB) model<sup>25</sup> that represents a typical 2D  $sp$ -band semiconductor in a trigonal lattice. The top of the valence band and bottom of the conduction band mainly consists of  $p$ - and  $s$ -state, respectively. An extrinsic  $s$ -state of alkali metal with appropriate energy is brought in to induce  $s$ - $p$  band inversion to form a TI phase; a generic phase diagram is constructed in the parameter space of energy levels and spin-orbit coupling (SOC). Then, using first-principles calculations, we demonstrate this approach for real materials by converting the semiconducting monolayer CuS and CuTe into TI via adsorbing Na and K respectively with a proper  $s$ -level energy, and CuSe

into TI via adsorbing a mixture of Na and K with a tuned  $s$ -level energy or by adsorbing either Na or K on a strained CuSe via a tuned  $p$ -level valence-band edge. Also, adsorption of Rb and Cs can work similarly.

We prescribe this concept of orbital design principle in a three-site(alkali metal adsorbate, cation and anion in a compound semiconductor) and four-band ( $s_1$  from adsorbate,  $s_2$ ,  $p_x$  and  $p_y$  from the 2D semiconductor) TB model. Expanding to the first-order of  $k$  around the  $\Gamma$  point, the spinless Hamiltonian reduces to

$$H = \begin{pmatrix} \varepsilon_{s_1} + 6t_{s_1s_1\sigma} & 3t_{s_1s_2\sigma} & -\frac{\sqrt{3}}{4}t_{s_1p\sigma}(ik_x + k_y) & -\frac{\sqrt{3}}{4}t_{s_1p\sigma}(ik_x - k_y) \\ & \varepsilon_{s_2} + 6t_{s_2s_2\sigma} & -\frac{\sqrt{3}}{2}t_{s_2p\sigma}(ik_x + k_y) & -\frac{\sqrt{3}}{2}t_{s_2p\sigma}(ik_x - k_y) \\ & & \varepsilon_p + 3(t_{pp\sigma} + t_{pp\pi}) + \lambda & 0 \\ & & & \varepsilon_p + 3(t_{pp\sigma} + t_{pp\pi}) - \lambda \end{pmatrix}, \quad (1)$$

where  $\varepsilon_{s_1}$ ,  $\varepsilon_{s_2}$  and  $\varepsilon_p$  are the on-site energies;  $t_{s_1s_1\sigma}$ ,  $t_{s_1s_2\sigma}$ ,  $t_{s_2s_2\sigma}$ ,  $t_{s_1p\sigma}$ ,  $t_{s_2p\sigma}$ ,  $t_{pp\sigma}$  and  $t_{pp\pi}$  are nearest-neighbor (NN) hopping parameters;  $\lambda$  is SOC strength;  $k_x$  and  $k_y$  are momenta along  $x$  and  $y$  direction respectively. The whole TB Hamiltonian is available in Note 1 in Supplementary Information.

At the  $\Gamma$  point, the four eigenvalues are  $E_{s_1} = \varepsilon_{s_1} + 6t_{s_1s_1\sigma}$ ,  $E_{s_2} = \varepsilon_{s_2} + 6t_{s_2s_2\sigma}$  and  $E_p^{\pm\lambda} = E_p \pm \lambda = \varepsilon_p + 3(t_{pp\sigma} + t_{pp\pi}) \pm \lambda$ , respectively.  $E_{s_1}$  and  $E_{s_2}$  are independent of SOC, while  $E_p$  are split by SOC with  $\Delta E_p^{\text{SOC}} = 2\lambda$ . As shown in Fig. 1(a), when the extrinsic  $s_1$  band with an appropriate energy is brought into the proximity of intrinsic  $s_2$   $p$ -bands of a 2D semiconductor, an  $s_1$ - $p$  band inversion can happen, resulting in topological phase transition to form the TI phase. Depending on whether the  $s_1$  band inverts with the upper or lower  $p_x/p_y$  band, there can be two types of TI phases as indicated by TI(A) and TI(B) in the right panel of Fig. 1(a).

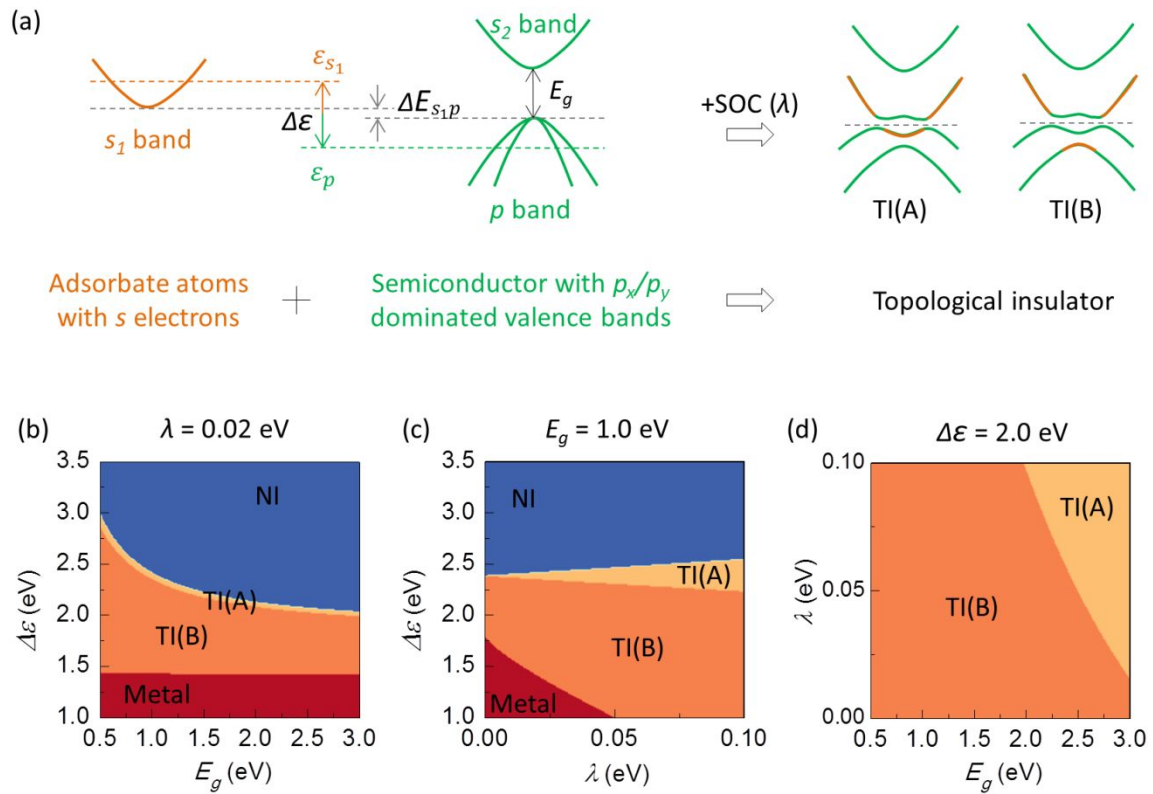


**Fig. 1** (a) Schematic illustration of orbital designed TIs from 2D semiconductors. The orange and green solid curves indicate the bands of the adsorbate atom and semiconductor, respectively. The dashed lines in the right panel indicate the Fermi level. TI(A) and TI(B) are defined for the  $s_1$  band inverting with the upper and lower  $p_x/p_y$  band, respectively. (b)-(d) Topological phase diagrams in the parameter space of  $\Delta\varepsilon$  and  $E_g$ ,  $\Delta\varepsilon$  and  $\lambda$ ,  $\lambda$  and  $E_g$ , respectively. The other parameters:  $t_{s_1s_1\sigma} = t_{s_1s_2\sigma} = t_{s_2s_2\sigma} = -0.25$  eV,  $t_{s_1p\sigma} = -0.5$  eV,  $t_{s_2p\sigma} = -0.1$  eV,  $t_{pp\sigma} = 0.1$  eV,  $t_{pp\pi} = 0.01$  eV and  $\theta = \pi/3$ .

To reveal how the orbital design principle works, we construct phase diagrams [Figs. 1(b)-(d) and Figs. S2-S4] of electronic structure in the parameter of  $\Delta\varepsilon = \varepsilon_{s_1} - \varepsilon_p$  (on-site energy difference between the adsorbate and the anion of semiconductor),  $E_g$  (band gap of semiconductor without SOC) and  $\lambda$ , based on the above TB model. With an increasing  $\Delta\varepsilon$  at given  $\lambda$  and  $E_g$  [Figs. 1(b) and (c)], the phase evolves from a metal, TI(B), TI(A), to a normal insulator (NI). The typical band structure of each phase is shown in Fig. S1. The  $s_1$ - $p$  band inversion may or may not exist in the absence of SOC.

When SOC is included, the degenerate  $p_x/p_y$  valence bands split. As illustrated in Fig. 1(d), this may result in a TI phase with an appropriate  $\Delta\varepsilon$ , which can be either a TI(A) or TI(B) phase. The condition for the occurrence of TI (A) or TI(B) phase is determined by relative magnitude of band splitting  $\Delta E_{s_1p} = E_{s_1} - E_p = \Delta\varepsilon - T$  (the  $s_1/p$  energy difference at the  $\Gamma$  point without considering SOC as indicated in Fig. 1(a);  $T$  is related to hopping parameters) and SOC gap  $\Delta E_p^{\text{SOC}}$ .<sup>3, 25</sup> The TI phase can only occur for  $\Delta E_{s_1p} < \Delta E_p^{\text{SOC}}$ , otherwise only NI exists. Furthermore, for  $\Delta E_{s_1p} < \Delta E_p^{\text{SOC}}$ , only TI(A) occurs for  $\Delta E_{s_1p} > 0$ , where the SOC induces an  $s_1-p$  band inversion similar to the case of small-gap quantum well;<sup>10</sup> for  $\Delta E_{s_1p} < 0$ , where the  $s_1-p$  bands are already inverted and the SOC simply opens a gap similar to graphene,<sup>9</sup> and depending on whether  $|\Delta E_{s_1p}|$  is smaller or bigger than  $\Delta E_p^{\text{SOC}}$ , either TI(A) or TI(B) occurs. Apparently, besides  $\Delta\varepsilon$ , the smaller  $E_g$  [Figs. 1(b) and S3] or bigger  $\lambda$  [Figs. 1(c) and S2] is, the larger the range of TI phase will be.

Given the understanding of the orbital design principle based on TB model, it is natural to ask whether it can be realized in real materials. Recently, experimental fabrication of monolayer CuSe,<sup>26, 27</sup> which possesses the  $p_x/p_y$ -dominated valence bands, has drawn our attention. The monolayer honeycomb monochalcogenides MX (M = Cu, Ag; X= S, Se, Te) family can all be viewed effectively as “hole-doped”  $sp$ -band 2D semiconductors, with one electron depleted per unit cell as shown in Fig. S5. It is expected that adsorption of one alkali atom per unit cell, which introduces one electron from  $s$ -orbital ( $s_1$ -state), will move the Fermi level up to the top of valence band and result in a semiconductor. Furthermore, if the energy of the  $s_1$ -state of alkali atom is right relative to the top of the valence  $p$ -band of semiconductor, the TI phase can be realized at certain condition based on the above design principle.

Therefore, the key is to identify the right alkali element with an appropriate  $s_1$ -state energy for a given 2D semiconductor, such as CuSe with the known valence  $p$ -band position and SOC strength. Because of the level repulsion, the relative position of final  $s_1$

and  $p$  bands is also affected by the bottom of the conduction  $s_2$  band. So, based on the above TB model, we construct a phase diagram for the  $\varepsilon_{s_1}$  of adsorbate in the parameter space of  $\varepsilon_{s_2}$  and  $\varepsilon_p$  of semiconductor, as shown in Fig. 2(a). It is found that the  $\varepsilon_{s_1}$  of the adsorbate decreases when the  $\varepsilon_{s_2}$  ( $\varepsilon_p$ ) of the cation (anion) in the compound semiconductor decreases (increases). Note that a decreased  $\varepsilon_{s_1}/\varepsilon_{s_2}$  and  $\varepsilon_p$  means an increasing ability of donating and accepting electrons, respectively. That is, with the ability of donating (accepting) electrons for cation (anion) increasing (decreasing) in semiconductor, the adsorbate to be chosen should have an increasing ability of donating electrons. Taking CuS, CuSe and CuTe as examples, which have the same cation but different anions, the ability of accepting electrons decreases from S, Se to Te, so the adsorbate should have an increasing ability of donating electrons.

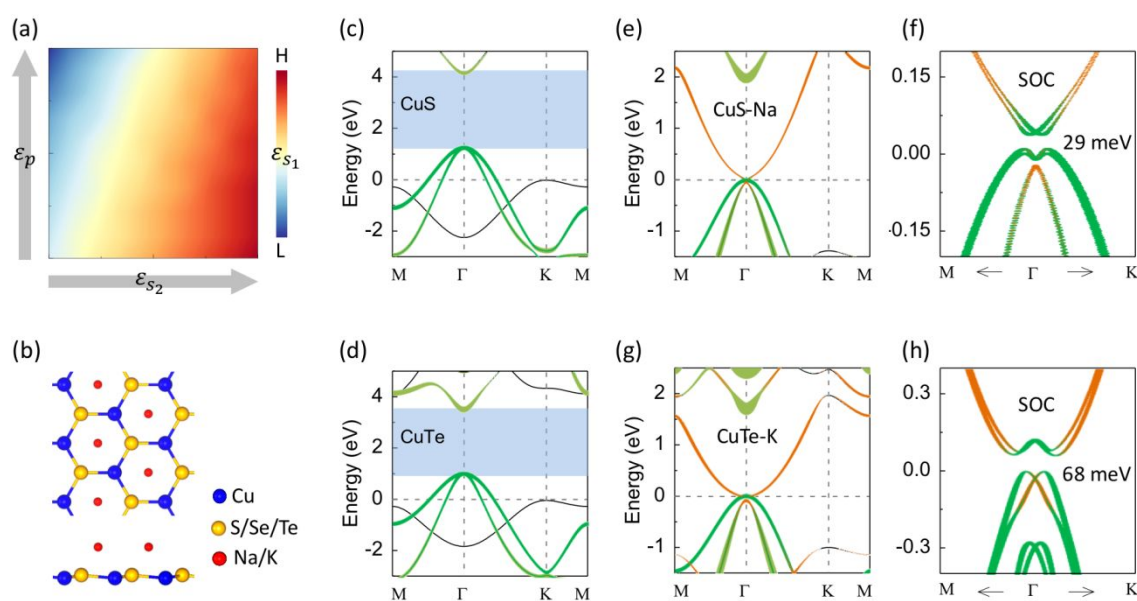


**Fig. 2** (a) Phase diagram of appropriate  $\varepsilon_{s_1}$  in the parameter space of  $\varepsilon_{s_2}$  and  $\varepsilon_p$ . The color indicates the value of  $\varepsilon_{s_1}$ . And an increased on-site energy ( $\varepsilon_{s_1}$ ,  $\varepsilon_{s_2}$  and  $\varepsilon_p$ ) means a decreasing ability of donating or accepting electrons. (b) Top and side views of monolayer MX-Y (M = Cu; X = S, Se, Te; Y = Na, K). (c)-(f) Projected band structures without SOC of CuS, CuTe, CuS-Na and CuTe-K, respectively. (g) and (h) Projected

band structures with SOC of CuS-Na and CuTe-K, respectively. The width of colored lines represents the contribution from different orbitals. The components of the X-s (X=Na, K) states are multiplied by a factor of 4 for clarity. The numbers indicate the band gap.

To confirm the above hypothesis, first-principles calculations (see Note 2 in Supplementary Information for details) have been performed for CuS, CuSe and CuTe with different alkali adsorbates. Alkali atom prefers to be adsorbed at the center of hexagon as shown in Fig. 2(b). The “*p*-type” semiconductors CuS and CuTe [Figs. 2(c) and (d)] have been successfully converted into TIs [Figs. 2(e)-(h)] via Na and K adsorption, respectively. Without considering SOC, the two degenerate  $p_x/p_y$  bands are exactly at the Fermi level. And the  $s_1$  band of adsorbate is below the  $p_x/p_y$  bands of host semiconductor near the  $\Gamma$  point, leading to “pre-existing” band inversion. When SOC is included, the degenerate  $p_x/p_y$  bands split with  $\Delta E_p^{SOC}$ , resulting in TI(B) and TI(A) phases for CuS-Na and CuTe-K, respectively. The ability of accepting electrons decreases from S to Te while the ability of donating electrons increases from Na to K, in good agreement with the prediction based on the orbital design principle.

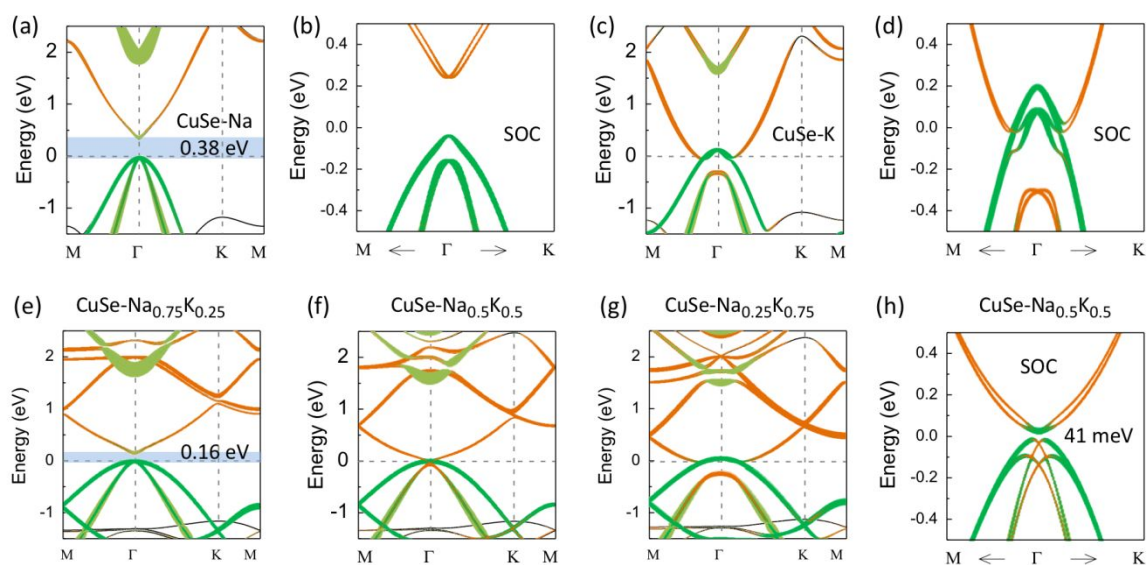


**Fig. 3** (a)-(d) Projected band structures without and with SOC of CuSe-Na and CuSe-K, respectively. (e)-(g) Projected band structures without SOC of CuSe-Na<sub>0.75</sub>K<sub>0.25</sub>, CuSe-Na<sub>0.5</sub>K<sub>0.5</sub> and CuSe-Na<sub>0.25</sub>K<sub>0.75</sub>, respectively. (h) Projected band structures with SOC of CuSe-Na<sub>0.5</sub>K<sub>0.5</sub>. The width of colored lines represents the contribution from different orbitals. The components of the X-s (X=Na, K) states are multiplied by a factor of 4 for clarity. The numbers indicate the band gap.

Next, we further investigate the band structures of CuSe-Na [Figs. 3(a) and (b)] and CuSe-K [Figs. 3(c) and (d)], which are NI and metal respectively. Because the ability of donating electrons for Se is between that for S and Te, the  $\epsilon_{s_1}$  of Na (K) is too big (small) to convert CuSe into TI. Thus, according to the phase diagram [Fig. 2(a)], the appropriate  $\epsilon_{s_1}$  is between that of Na and K, indicating that adsorbing a mixture of Na and K with a tuned  $s_1$ -level energy may convert CuSe into TI. This is indeed confirmed by calculations of CuSe via adsorbing mixtures of Na and K with different ratios as shown in Figs. 3(e)-(g). With the Na/K ratio decreasing, the  $s_1$  band moves downward at the  $\Gamma$  point and the band structure evolves from CuSe-Na to CuSe-K with the band inversion occurring at CuSe-Na<sub>0.5</sub>K<sub>0.5</sub>. When SOC is included, CuSe-Na<sub>0.5</sub>K<sub>0.5</sub> is found a TI possessing a non-trivial gap of 41 meV as shown in Fig. 3(h).

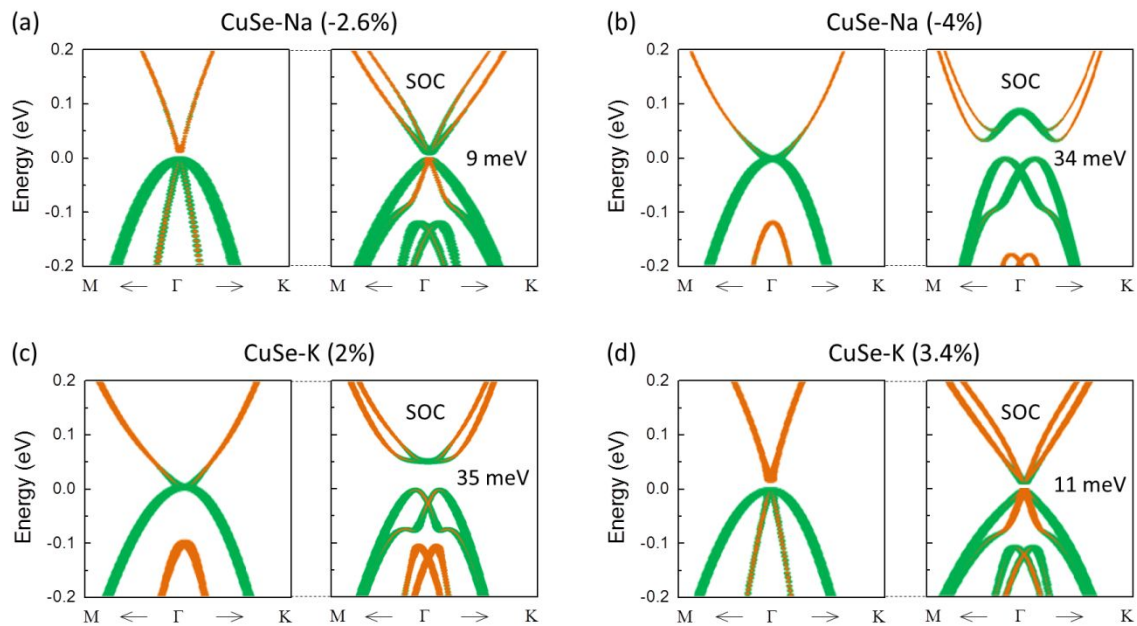


**Fig. 4** (a) and (b) Projected band structures of CuSe-Na with -2.6% and -4% compressive strain, respectively. (c) and (d) Projected band structures of CuSe-K with 2% and 3.4% tensile strain, respectively. The width of colored lines represents the contribution from different orbitals. The components of the X-s (X= Na, K) states are multiplied by a factor of 4 for clarity. The numbers indicate the band gap.

Besides tuning the  $s_1$  band via adsorbing different alkali elements, one can also slightly tune the  $p_x/p_y$  valence bands of host semiconductor via strain so as to achieve a desired  $\Delta E_{s_1p}$ . For example, CuSe-Na is a NI. By applying a compressive strain, the relative energy of  $s_1$  band to the  $p_x/p_y$  bands decreases near the  $\Gamma$  point (Fig. S6). Then, the phase evolves from a NI, TI(A), TI(B) to a metal with the increasing strain (Fig. S6). The specific band structure of TI(A) and TI(B) phases are shown in Figs. 4(a) and (b), respectively, for CuSe-Na with -2.6% and -4% compressive strain. To convert CuSe-Na into TI, the range of compressive strain is about -2.3% ~ -4.5%.

Similarly, CuSe-K is a metal. By applying a tensile strain, the relative energy of  $s_1$  band to the  $p_x/p_y$  bands increases near the  $\Gamma$  point (Fig. S7). The phase evolves from a metal, TI(B), TI(A) to a NI with the increasing strain (Fig. S7). The specific band structure of TI(B) and TI(A) phases are shown in Figs. 4(c) and (d), respectively, for

CuSe-K with 2% and 3.4% tensile strain. To convert CuSe-K into TI, the range of tensile strain is about 1% ~ 3.6%. To confirm the  $s_1$ - $p$  inverted bands display a topological insulating states, taking CuSe-K with 3% tensile strain as an example, we calculated its nontrivial edge states as shown in Fig. S8.

We have also tried out using Rb and Cs as adsorbates and found that CuSe-Cs, CuTe-Rb and CuTe-Cs are 2D TIs, as shown in Fig. S9. Furthermore, taking the alkali atom adsorbed CuX (X = S, Se, Te) monolayers as examples, we further checked their stability. The calculated phonon dispersion of these monolayers are shown in Fig. S10. There is no imaginary frequency mode in the whole Brillouinzone, indicating that they are dynamically stable.

In conclusion, we propose a novel approach underlined by an orbital design principle, to rationally convert 2D  $sp$ -band semiconductors into TIs. We envision that this approach is generally applicable to a large number of 2D material databases. As prototypical examples, the feasibility of the approach is confirmed by first-principles calculations of monolayer CuX (X = S, Se, Te) via adsorbing alkali atoms. Depending on the desired relative position of extrinsic  $s$ -band of alkali atoms to the intrinsic top of  $p$ -valence band of host, a mixture of alkali atoms and either tensile or compressive strains may be needed. Our findings not only enrich 2D TIs with new material classes but also revive the discovery of TIs by predictive material designs.

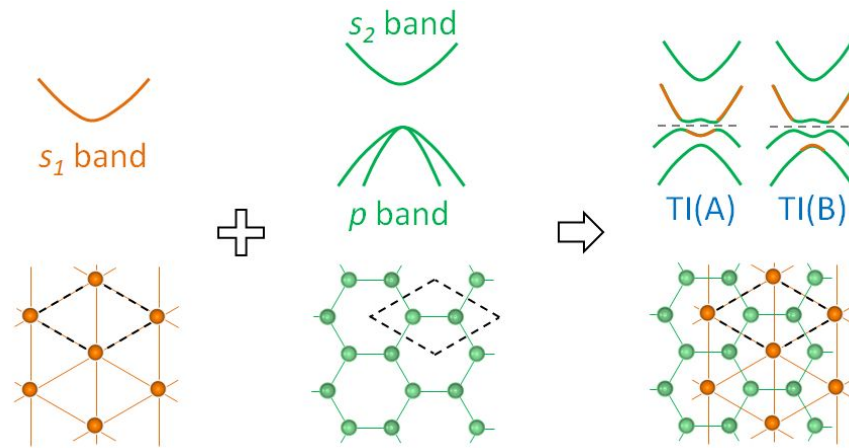
## ACKNOWLEDGEMENTS

This work was financially supported by National Key Research and Development Projects of China (2016YFA0202300), Strategic Priority Research Program of Chinese Academy of Sciences (Grant Nos. XDB30000000 and XDB07030100), the National Natural Science Foundation of China (No. 51872284 and 61888102), the International Partnership Program of Chinese Academy of Sciences (No. 112111KYSB20160061), and the CAS Pioneer Hundred Talents Program, Beijing Nova Program (No. Z181100006218023). This project was also supported by the CAS Key Laboratory of Vacuum Physics and the Beijing Key Laboratory for Nanomaterials and Nanodevices. G.S. and F.L. at Utah acknowledge the support from US-DOE (Grant No. DE-FG02-04ER46148).

## References

1. S. D. Sarma, S. Adam, E. H. Hwang and E. Rossi, *Rev. Mod. Phys.*, 2011, **83**, 407-470.
2. A. K. Geim and I. V. Grigorieva, *Nature*, 2013, **499**, 419-425.
3. Z. F. Wang, K.-H. Jin and F. Liu, *WIREs Comput. Mol. Sci.*, 2017, **7**, e1304.
4. G. Li, Y. Y. Zhang, H. Guo, L. Huang, H. Lu, X. Lin, Y. L. Wang, S. Du and H. J. Gao, *Chem. Soc. Rev.*, 2018, **47**, 6073-6100.
5. K. S. Novoselov, A. K. Geim, S. V. Morozov, D. Jiang, M. I. Katsnelson, I. V. Grigorieva, S. V. Dubonos and A. A. Firsov, *Nature*, 2005, **438**, 197-200.
6. Y. B. Zhang, Y. W. Tan, H. L. Stormer and P. Kim, *Nature*, 2005, **438**, 201-204.
7. F. Xia, H. Wang and Y. Jia, *Nat. Commun.*, 2014, **5**, 4458.
8. K. S. Novoselov, D. Jiang, F. Schedin, T. J. Booth, V. V. Khotkevich, S. V. Morozov and A. K. Geim, *Proc. Natl. Acad. Sci. U.S.A.*, 2005, **102**, 10451-10453.
9. C. L. Kane and E. J. Mele, *Phys. Rev. Lett.*, 2005, **95**, 226801.
10. B. A. Bernevig, T. L. Hughes and S. C. Zhang, *Science*, 2006, **314**, 1757-1761.
11. F. Reis, G. Li, L. Dudy, M. Bauernfeind, S. Glass, W. Hanke, R. Thomale, J. Schäfer and R. Claessen, *Science*, 2017, **357**, 287.
12. L. Kou, Y. Ma, Z. Sun, T. Heine and C. Chen, *J. Phys. Chem. Lett.*, 2017, **8**, 1905-1919.
13. Q.-Y. Wang, Z. Li, W.-H. Zhang, Z.-C. Zhang, J.-S. Zhang, W. Li, H. Ding, Y.-B. Ou, P. Deng, K. Chang, J. Wen, C.-L. Song, K. He, J.-F. Jia, S.-H. Ji, Y.-Y. Wang, L.-L. Wang, X. Chen, X.-C. Ma and Q.-K. Xue, *Chin. Phys. Lett.*, 2012, **29**, 037402.
14. B. Huang, G. Clark, E. Navarro-Moratalla, D. R. Klein, R. Cheng, K. L. Seyler, D. Zhong, E. Schmidgall, M. A. McGuire, D. H. Cobden, W. Yao, D. Xiao, P. Jarillo-Herrero and X. Xu, *Nature*, 2017, **546**, 270-273.
15. Z. F. Wang, Z. Liu and F. Liu, *Phys. Rev. Lett.*, 2013, **110**, 196801.
16. Z. F. Wang, Z. Liu and F. Liu, *Nat. Commun.*, 2013, **4**, 1471.
17. X. Zhang, Y. Zhou, B. Cui, M. Zhao and F. Liu, *Nano Lett.*, 2017, **17**, 6166-6170.

18. E. Jin, M. Asada, Q. Xu, S. Dalapati, M. A. Addicoat, M. A. Brady, H. Xu, T. Nakamura, T. Heine, Q. Chen and D. Jiang, *Science*, 2017, **357**, 673–676.
19. C. Si, Z. Liu, W. Duan and F. Liu, *Phys. Rev. Lett.*, 2013, **111**, 196802.
20. B. Huang, M. Yoon, B. G. Sumpter, S. H. Wei and F. Liu, *Phys. Rev. Lett.*, 2015, **115**, 126806.
21. C. Tan, X. Cao, X. J. Wu, Q. He, J. Yang, X. Zhang, J. Chen, W. Zhao, S. Han, G. H. Nam, M. Sindoro and H. Zhang, *Chem. Rev.*, 2017, **117**, 6225–6331.
22. Z. F. Wang, Y. Zhang and F. Liu, *Phys. Rev. B*, 2011, **83**, 041403.
23. Y. Zhang and F. Liu, *Appl. Phys. Lett.*, 2011, **99**, 241908.
24. C. Si, Z. Sun and F. Liu, *Nanoscale*, 2016, **8**, 3207–3217.
25. Z. F. Wang, K. H. Jin and F. Liu, *Nat. Commun.*, 2016, **7**, 12746.
26. X. Lin, J. C. Lu, Y. Shao, Y. Y. Zhang, X. Wu, J. B. Pan, L. Gao, S. Y. Zhu, K. Qian, Y. F. Zhang, D. L. Bao, L. F. Li, Y. Q. Wang, Z. L. Liu, J. T. Sun, T. Lei, C. Liu, J. O. Wang, K. Ibrahim, D. N. Leonard, W. Zhou, H. M. Guo, Y. L. Wang, S. X. Du, S. T. Pantelides and H. J. Gao, *Nat. Mater.*, 2017, **16**, 717–721.
27. L. Gao, J. T. Sun, J. C. Lu, H. Li, K. Qian, S. Zhang, Y. Y. Zhang, T. Qian, H. Ding, X. Lin, S. Du and H. J. Gao, *Adv. Mater.*, 2018, **30**, 1707055.



The orbital design approach to convert two-dimensional semiconductors to topological insulators via selective atomic adsorption or strain are proposed.